Short note: event-consistent smoothing of kinematic wavefield attributes for stacking and inversion

J. Mann and E. Duveneck

email: *Juergen.Mann@gpi.uka.de*
keywords: *CRS stack, wavefield attributes, smoothing*

ABSTRACT

The kinematic wavefield attributes used in the stacking operator of the Common-Reflection-Surface stack offer a variety of applications in addition to the original task, the simulation of a stacked section. Examples are the determination of smooth or blocky velocity models, an attribute-based time migration, or the estimation of properties like the geometrical spreading factor or the size of the projected Fresnel zone. All these applications rely on a sufficient accuracy of the wavefield attributes. However, the attributes actually determined by means of coherence analysis in the seismic reflection prestack data are subject to fluctuations due to noise as well as to outliers related to deficiencies of the employed search strategies. To overcome these problems, we introduce a smoothing algorithm which removes such fluctuations and outliers in an event-consistent manner and in accordance with theory.

INTRODUCTION

The Common-Reflection-Surface (CRS) stack was originally developed to simulate 2D zero-offset (ZO) sections as an alternative to conventional methods like the sequence normal moveout (NMO) correction/dip moveout (DMO)correction/stack. Meanwhile, the approach has been generalized in various directions, e. g. to the 3D case, finite-offset situations, or acquisition surfaces with topography.

The CRS stack can be seen as a generalized high-density velocity analysis tool based on coherence analyses in the prestack data. Each set of kinematic wavefield attributes is determined independently of neighboring ZO samples. Although a high-density analysis is desirable for obvious reasons, the kinematic wavefield attributes determined in this manner suffer from two general problems: on the one hand, we observe fluctuations of the attributes due to the noise in the data. Theoretical considerations show, however, that the attributes can only vary smoothly along the reflection events and are virtually constant along the seismic wavelet. Thus, fluctuations of the wavefield attributes do not represent useful information about the parameterized reflections events and should be removed prior to subsequent applications of the attributes. On the other hand, the implemented search strategies sometimes fail to detect the searched-for (usually global) coherence maxima associated with the optimum stacking operators and their corresponding sets of wavefield attributes. This causes outliers that deteriorate the performance of local optimization steps used to refine the wavefield attributes, as well as any subsequent application of the kinematic wavefield attributes. In this contribution, we introduce a smoothing algorithm for the kinematic wavefield attributes that removes fluctuations due to noise as well as outliers in accordance with theory in an event-consistent manner. The successful application of the smoothing algorithm is demonstrated in the case studies presented by Hertweck et al. (2003) and Heilmann et al. (2003) in this report.

IMPLEMENTATION

To perform an event-consistent smoothing of the attributes, we have to consider the local orientation of the reflection event and the reliability of its associated wavefield attributes at each ZO sample (x_0, t_0). The orientation can be derived from the CRS wavefield attribute α, i. e., the emergence angle of the normal ray: the horizontal slowness p (or half of the first spatial derivative of ZO traveltime) is simply given by

$$p = \frac{1}{2}\frac{\partial t}{\partial x_\mathrm{m}}\bigg|_{(x_\mathrm{m}=x_0,h=0)} = \frac{\sin\alpha}{v_0}\,,$$

where v_0 denotes the near-surface velocity used for the CRS stack and x_m and h are the midpoint and half-offset coordinates, respectively. Note that p itself is independent of the near-surface velocity. Thus, the following considerations also apply in case of a wrong value of v_0, although α no longer represents the actual emergence angle in such situations.

The reliability of the attributes for a ZO sample can be evaluated by means of the coherence value obtained along the corresponding stacking operator in the prestack data. Low coherence values might occur due to several reasons:

- the ZO sample is not located on a reflection event. In such situations, no significant contribution to the stack can be expected and the wavefield attributes are meaningless.
- data with low signal-to-noise ratio. The wavefield attributes are relevant, but subject to fluctuations not supported by the theory.
- failure of the search strategy to detect the global coherence maximum. This usually leads to isolated outliers in the attribute sections.
- complex wavefields with strongly non-hyperbolic events. In such cases, the aperture choice for the CRS stack should be reconsidered. The attributes might be misleading.

In the first case, no useful smoothing is possible and necessary. In the remaining cases, an appropriate smoothing of the attributes allows to remove the fluctuations due to the noise in the data as well as outliers. However, limitations due to the second-order approximation of traveltime with respect to x_m and h cannot be overcome in this way. With the help of the CRS-stack results, a minimum coherence value S_min can be estimated to identify ZO samples located on actual reflection events. Only ZO samples associated with coherence values $S > S_\text{min}$ will contribute to the smoothing process.

The CRS wavefield attributes are related to the first and second spatial derivatives of the traveltime in the prestack data. As long as we deal with situations where zero-order ray theory is valid, these derivatives can only vary smoothly along the reflection events. In the time direction, i. e., along the seismic wavelet, the wavefield attributes are even virtually constant (Mann and Höcht, 2003). Thus, it is fully consistent with the theory to attribute all fluctuations and outliers along reliably detected events to noise in the data and failures of the optimization strategy. There is no reason for any loss of relevant information about the reflection events due to appropriately applied smoothing of the wavefield attributes.

One particular problem has to be considered in addition: conflicting dip situations. Irrespective whether such situations have been explicitly handled during the CRS stack, we have to expect that the wavefield attributes for neighboring ZO samples might characterize different reflection events. Of course, the wavefield attributes of different events must not be mixed by the smoothing algorithm. To avoid this, neighboring wavefield attributes are only included in the smoothing process for ZO samples where the emergence angle deviates only by a small variation $\Delta\alpha_\text{max}$ with respect to the emergence angle at the reference location. In this way, the attributes associated with different intersecting reflection events remain independent of each other.

User-defined parameters

The smoothing algorithm in its current implementation requires a set of user-defined parameters:

- spatial and temporal extension of the moving smoothing window
- a coherence threshold S_min to identify ZO samples located on reliably detected reflection events
- an angle variation threshold $\Delta\alpha_\text{max}$ to avoid the mixing of different events
- a fraction $0 < f \leq 1$ to control the combination of median filter and averaging (see below)

Smoothing algorithm

The basic processing steps to calculate the smoothed wavefield attributes for a given ZO location read as follows:

- tilt the smoothing window according to the local dip $2p$
- reject all points within the window with $S < S_{\text{min}}$ to avoid the use of unreliable attributes
- reject all points within the window with $\Delta\alpha > \Delta\alpha_{\text{max}}$ to avoid a mixing of attributes associated with independent reflection events
- separately compute the average of each attribute for a fraction f of the remaining data points centered around the respective median of its distribution

If no data points remain for averaging after the application of the above-mentioned criteria, the original wavefield attributes are used. Note that for the normal wavefront, the curvature $1/R_{\text{N}}$ is smoothed rather than the radius of curvature R_{N}.

DATA EXAMPLES

As mentioned above, the proposed smoothing algorithm was also used for the case studies presented by Hertweck et al. (2003) and Heilmann et al. (2003) in this report. Therefore, we only present some details of results obtained for different real data sets to demonstrate the effect of the smoothing algorithm.

Firstly, we discuss the effect of the proposed smoothing algorithm on the wavefield attributes themselves. As the emergence angle α and the radius of the NIP wavefront R_{NIP} are the relevant parameters for many applications, especially the determination of a velocity model (Duveneck, 2002), we restrict ourselves to these two parameters for the sake of brevity. Figures 1 and 2 show two subsets of the α and R_{NIP} sections associated with a real data example where the prestack data were of very low signal-to-noise ratio. In the top rows, the original attribute sections as obtained by the CRS stack before the final local optimization, also called initial CRS stack, are shown. The middle rows show the original attribute sections overlain with a mask based on the coherence values. This removes the strongly fluctuating and meaningless attributes between the reflection events and serves for display purposes, only. In the bottom rows of Figures 1 and 2, the attribute sections after event-consistent smoothing are displayed, again overlain with the coherence-based mask.

As expected, outliers and high-frequency fluctuations of the attributes are almost completely removed in both examples without introducing any artifical structures. Furthermore, the second example (Figure 2) clearly demonstrates the ability of the smoothing algorithm to keep the attributes of different reflection events strictly separated: no mixing or blurring of the attributes along boundaries between reflection events with different dips can be observed.

We will now investigate the effect of the attribute smoothing on the CRS stacked sections. In Figure 3, two details of a simulated ZO section are depicted for areas in the vicinity of fault zones. Again, the results of the initial CRS stack are shown, on the left hand side with the original attributes, on the right hand side with the smoothed attributes. Note that this does not yet represent the final CRS stack results, which are usually further improved by means of a local multi-parameter optimization. Of course, this local optimization also benefits from the smoothed attributes as they provide better initial values. However, our aim here is to present the direct effect of the attribute smoothing, only.

The stack results based on the smoothed attributes show a significantly higher continuity of the reflection events. Several events can be clearly identified which are highly disrupted in the original stack results. Isolated outliers visible as speckles in the original stack sections have been largely removed. This is advantageous for further processing steps like post-stack migration. Such high-frequency speckles are problematic for all processes applied in the frequency domain as they appear at the Nyquist frequency. In Kirchhoff migration, the speckles, if not removed, would systematically lead to migration artifacts.

CONCLUSION

We introduced an event-consistent smoothing algorithm for the kinematic wavefield attributes obtained by the CRS stack. Application examples showed that the proposed algorithm is able to remove physically

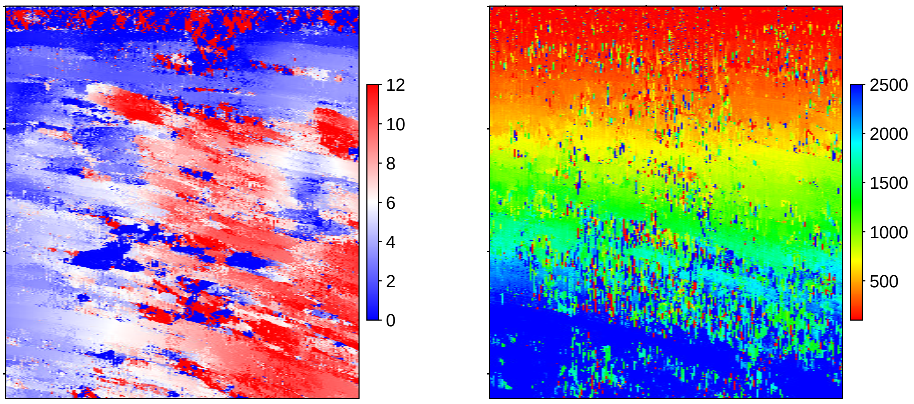

(a) Original emergence angle [°]

(b) Original NIP radius [m]

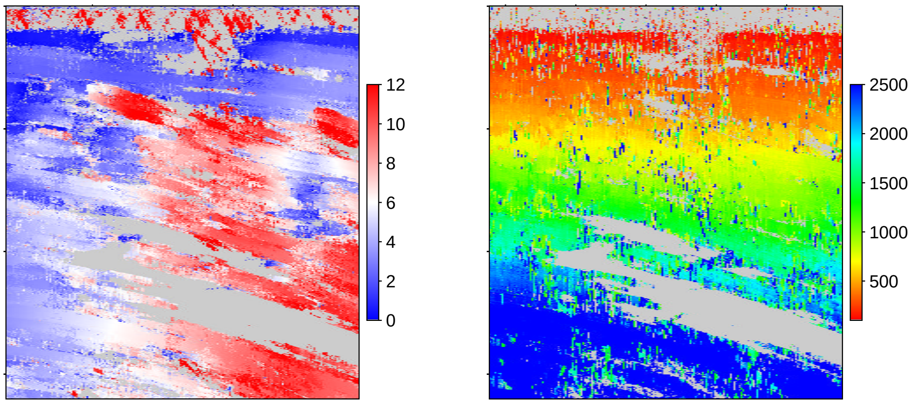

(c) Masked emergence angle [°]

(d) Masked NIP radius [m]

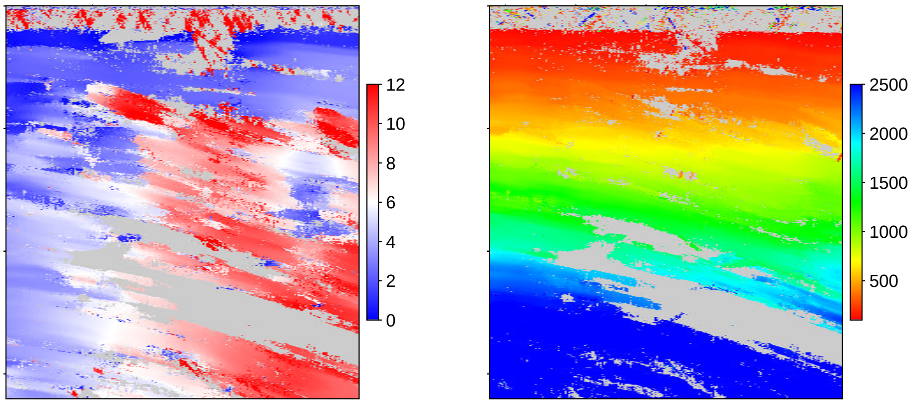

(e) Smoothed emergence angle [°]

(f) Smoothed NIP radius [m]

Figure 1: Wavefield attributes α and R_{NIP} for a real data example. See main text for details.

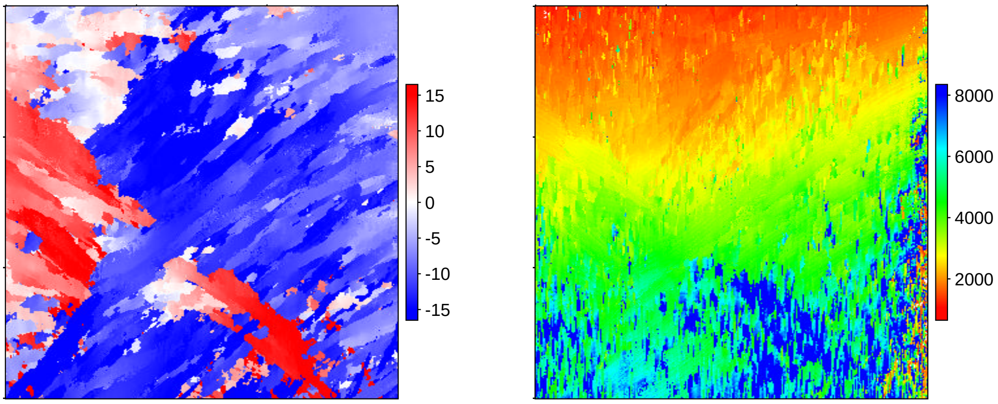

(a) Original emergence angle $[^\circ]$ **(b)** Original NIP radius [m]

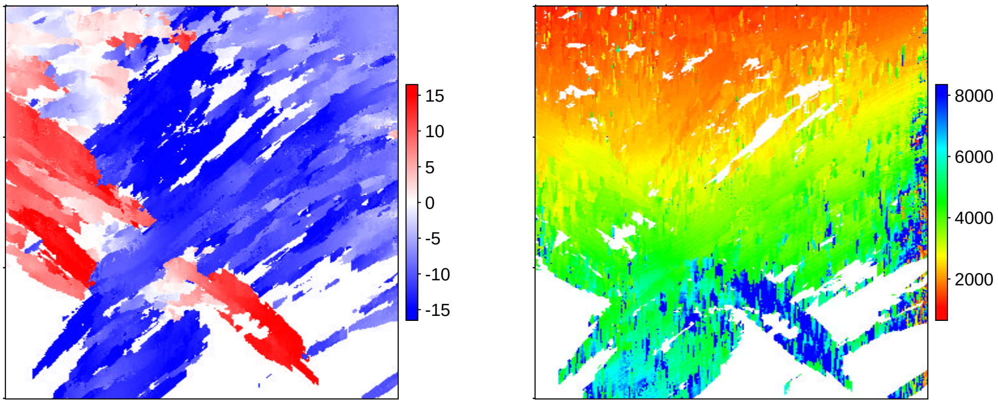

(c) Masked emergence angle $[^\circ]$ **(d)** Masked NIP radius [m]

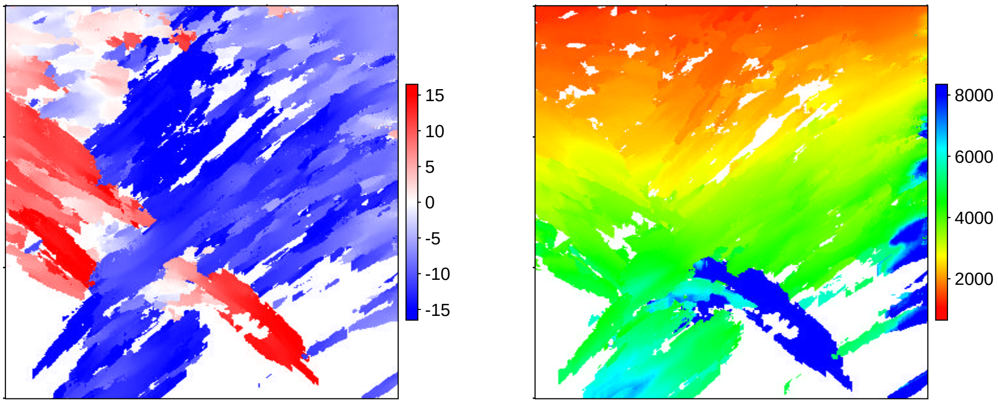

(e) Smoothed emergence angle $[^\circ]$ **(f)** Smoothed NIP radius [m]

Figure 2: Wavefield attributes α and R_{NIP} for a real data example. See main text for details.

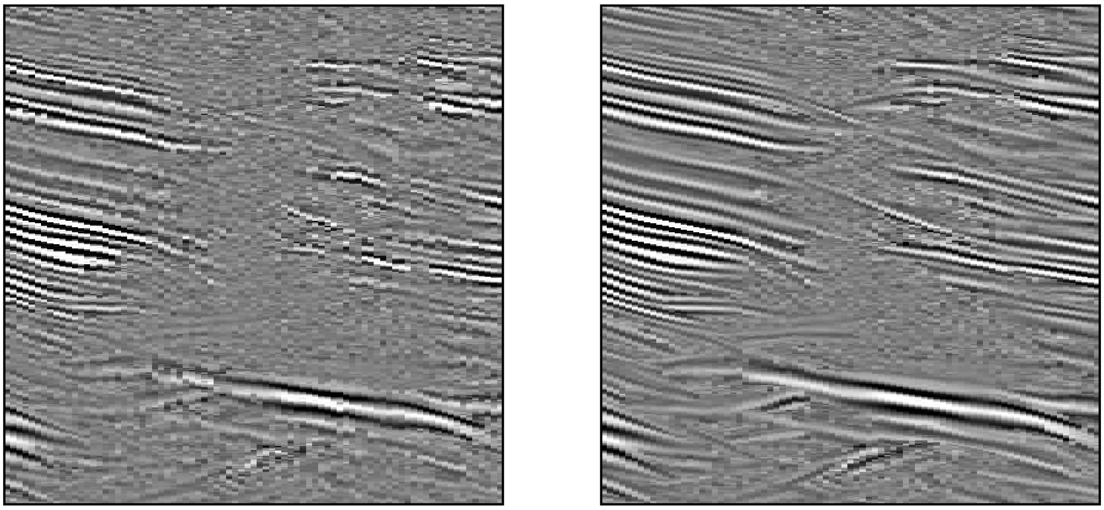

(a) Original stack

(b) Stack with smoothed attributes

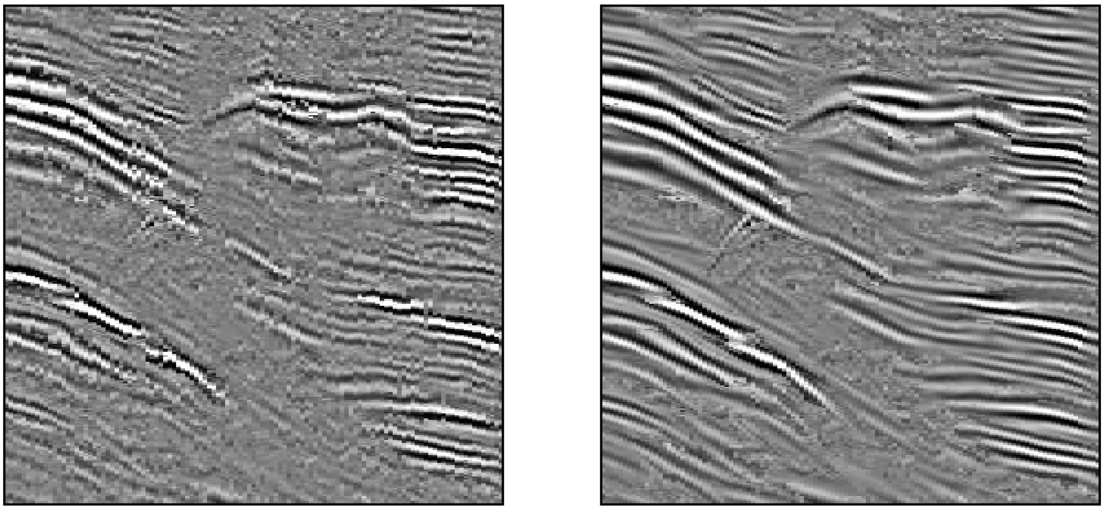

(c) Original stack

(d) Stack with smoothed attributes

Figure 3: Details of a CRS stacked section before/after smoothing of the attributes. See main text for details.

unreasonable outliers and fluctuations from the attribute sections without reducing the spatial resolution of interpretable properties of the reflection events and without any cross-talk between intersecting events in conflicting dip situations.

REFERENCES

Duveneck, E. (2002). Tomographic velocity model inversion with CRS attributes. *Annual Report, Wave Inversion Technology Consortium*, pages 92–106.

Mann, J. and Höcht, G. (2003). Pulse stretch effects in the context of data-driven imaging methods. In *65th Mtg. Eur. Assn. Geosci. Eng., Extended Abstracts*, Session P007.